Reaction Chemistry & Engineering

PAPER

View Article Online
View Journal | View Issue

Cite this: *React. Chem. Eng.*, 2016, **1**, 508

Adenine as an organocatalyst for the ring-opening polymerization of lactide: scope, mechanism and access to adenine-functionalized polylactide†

Guilherme Nogueira,[ab] Audrey Favrelle,[a] Marc Bria,[c] João P. Prates Ramalho,[d] Paulo J. Mendes,[d] Andreia Valente[b] and Philippe Zinck*[a]

Nucleobase-functionalized polymers are widely used in the fields of supramolecular chemistry and self-assembly, and their development for biomedical applications is also an area of interest. They are usually synthesized by tedious multistep procedures. In this study, we assess adenine as an organoinitiator/organocatalyst for the ring-opening polymerization of lactide. L-Lactide can be quantitatively polymerized in the presence of adenine. Reaction conditions involving short reaction times and relatively low temperatures enable the access to adenine end-capped polylactide in a simple one-step procedure, in bulk, without additional catalyst. DFT calculations show that the polymerization occurs *via* hydrogen bond catalysis. The mechanism involves (i) a hydrogen bond between the NH9 of adenine and the carbonyl moiety of lactide, leading to an electron deficient carbon atom, and (ii) a second hydrogen bond between the N3 of adenine and the NH_2 of a second adenine molecule, followed by a nucleophilic attack of the latter activated amine on the former electron deficient carbon on the monomer. For longer reaction times and higher temperatures, macrocyclic species are formed, and a mechanism involving the imidazole ring of adenine is proposed based on literature studies. Depending on the reaction conditions, adenine can thus be considered as an organoinitiator or an organocatalyst for the ring-opening polymerization of lactide.

Received 18th March 2016,
Accepted 23rd June 2016

DOI: 10.1039/c6re00061d

rsc.li/reaction-engineering

Introduction

The use of organic molecules as catalysts for the ring-opening polymerization of cyclic esters and carbonates has gained much interest these past years.[1–5] Of particular interest is the functionalization of biocompatible aliphatic polyesters *via* organocatalysis, as this leads to macromolecular objects of interest for biomedical applications that do not contain any metallic traces. Monosaccharide[6–10] and cyclodextrin[8–13] end-capped polylactides and polylactones, together with other kinds of star-shaped polyesters,[14] were synthesized *via* organocatalysis. The use of a molecule of biological interest as an organoinitiator, *i.e.* a molecule able to initiate the ring-opening polymerization of cyclic esters without any cocatalyst, is even more interesting, as the resulting material will not contain any catalytic residue. Cyclodextrins, for example, were reported to initiate the ring-opening oligomerization of lactones[15–17] and lactides[18] without additional catalysts. Amino acids were also reported as organoinitiators for the polymerization of cyclic esters. L-Arginine and L-citrulline were reported to initiate the ring-opening polymerization of ε-caprolactone and L-lactide at 160 °C, yielding the resulting end-capped polyester.[19]

Nucleobase-functionalized polymers have been widely used in the field of supramolecular chemistry for accessing complementary hydrogen-bonding self-assembly polymers, having various applications, notably in the biomedical field.[20] These biological molecules are usually derivatized and then introduced in the polymer backbone through direct polymerization, acting as the monomer[21–23] or the initiator,[24,25] or by post-functionalization[26–30] of the polymer backbone. The synthesis of (adenine and uracil)-functionalized poly(ε-caprolactone) was for example reported by combining ring-opening polymerization and Michael addition.[24] The adenine molecule (Scheme 1) was derivatized by the heterocyclic secondary amine group (NH9) and used as the initiator of the polymerization along with

[a] *Unité de Catalyse et Chimie du Solide (UCCS), UMR CNRS 8181, ENSCL, Université de Lille, F-59000 Lille, France. E-mail: philippe.zinck@univ-lille1.fr*
[b] *Centro de Química Estrutural, Faculdade de Ciências da Universidade de Lisboa, Campo Grande, 1749-016 Lisboa, Portugal*
[c] *Centre Commun de Mesure RMN, Université de Lille, F-59000 Lille, France*
[d] *Departamento de Química and Centro de Química de Évora, Escola de Ciências e Tecnologia, Universidade de Évora, Rua Romão Ramalho, 59, 7000-671 Évora, Portugal*

† Electronic supplementary information (ESI) available. See DOI: 10.1039/c6re00061d

triethylaluminum as a co-initiator in DMSO. In another example, star-shaped poly(D,L-lactide) containing peripheral complementary hydrogen-bonding sites was obtained by the post-functionalization of a four-arm derivatized polymer chain end with adenine or thymine nucleobases through a Michael addition reaction.[26]

N-heterocyclic bases such as amidines, guanidines or pyridine derivatives have been widely studied in polymerization organocatalysis. They show excellent performances for the ring-opening polymerization of cyclic esters.[31–36] Even if adenine has a low pK_a value (p$K_{a,adenineH^+}$ = 4.3), we envisioned its use as an organoinitiator for the ring-opening polymerization of cyclic esters in order to access adenine end-capped biocompatible aliphatic polyesters. The amine group is indeed able to initiate the ring-opening polymerization of cyclic esters.[37] Such an approach would be of great relevance in the field of molecules for medical applications, reducing the reaction steps and avoiding unwanted metallic traces from the final formulation. This might be particularly relevant in the field of anticancer drugs[10] where one can rationalize the synthesis of polymer–metal conjugates that would benefit from the enhanced permeation and retention effect[38] *in vivo* due to the higher molecular weight introduced by the use of a polymeric macroligand (passive targeting) and by the use of a nucleobase (adenine) which receptors (adenosine receptors) are overexpressed in many types of cancer (active targeting).[39] Adenine has indeed an important role in the organism since it is present as a constituent of important energy resources such as adenosine triphosphate (ATP), nicotinamide adenine dinucleotide (NAD) or flavin adenine dinucleotide (FAD). In addition, since there is evidence that this purine derivative is recognized by the adenosine receptors,[40] the rationale behind the synthesis of polymer–metal conjugates bearing adenine moieties is very relevant. We assess herein adenine as an organoinitiator for the ring-opening polymerization of L-lactide and report, after optimization of the reaction, the formation of adenine end-capped polylactide using a simple, one-step procedure in bulk. The reaction mechanism is discussed based on MALDI ToF analyses, DFT studies and results from the literature.

Experimental

Materials

L-Lactide (98%), adenine (99%) and 4-aminopyridine (99%) were purchased from Aldrich. They were co-evaporated three times with toluene, and L-lactide was further sublimated under vacuum at 85 °C. The products were stored in a glove box.

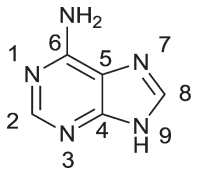

Scheme 1 Adenine.

Polymerization

In a typical polymerization procedure, certain amounts of adenine (or 4-aminopyridine for entry 12) and L-lactide were added into a flask in a glove-box. The closed reaction flask was completely immersed in a preheated oil bath, and the mixture was allowed to react at a given temperature for a given time. The viscous reaction product was dissolved in a small amount of dichloromethane, and a sample of the crude product was taken for ^{1}H-NMR analysis. The solution was precipitated into a cold mixture of methanol/distilled water [200 mL (v/v) (50/50)]. After precipitation, the supernatant was decanted, and the resultant material was dried under vacuum at room temperature until constant weight. For a L-lactide/adenine ratio of 20, where the initiation efficiency is not quantitative (see discussion in the text), the dichloromethane solution was filtered with a syringe filter before precipitation in order to remove unreacted adenine.

Measurements

NMR spectra were recorded on a Bruker AV 300 MHz spectrometer in DMSO-d_6. Approximately 3 mg of sample were directly dissolved into the NMR tube in 0.5 mL of solvent for ^{1}H NMR. The chemical shifts given in parts per million (ppm) were calibrated using the residual resonances of the deuterated solvent. The conversion of the polymerization of lactide was determined by the integration of the –CH proton of lactide (5.42 ppm) *vs.* the –CH proton of polylactide (5.18 ppm).

Fourier transform infrared spectroscopy (FTIR) spectra were recorded using a Shimadzu IRAffinity-1 FTIR spectrophotometer with KBr pellets in air at room temperature. Gel permeation chromatography (GPC) was performed in THF as an eluent at 40 °C using a Waters SIS HPLC pump, a Waters 2414 refractometer and Waters Styragel columns HR3 and HR4. The calibration was performed using polystyrene standards. A correction factor of 0.58 was applied for the determination of the number-average molecular weight of poly(L-lactide).[41] Matrix assisted laser desorption ionization mass spectrometry (MALDI-ToF-MS) was performed using an Ultraflex II spectrometer (Bruker). The instrument was operated in reflector positive-ion mode. The samples were prepared by taking 2 μL of a THF solution of the polymer (10 mg mL^{-1}) and adding this to 16 μL of 1,8-dihydroxy-9(10*H*)-anthracenone (dithranol, 10 mg mL^{-1} in THF) to which 2 μL of CF_3SO_3Ag (2 mg mL^{-1} in THF) had been added. A 1 μL portion of this mixture was applied to the target, and 50–100 single shot spectra were accumulated. The given masses represent the average masses of the Ag^+ adducts.

Calculation details

All calculations were performed within the framework of density functional theory (DFT) using the Gaussian 09 package.[42]

For all reactants, products and transition states, geometries were obtained by DFT from optimizations using the hybrid meta-GGA M06-2X[43] functional with the 6-31+G(d,p) basis set. Frequency analysis was subsequently performed confirming each optimized geometry as an energy minimum for reactants and products, by the absence of imaginary frequencies and for the transition states by possessing a single imaginary frequency. The energies reported herein are corrected for the zero-point vibrational effects. In order to simplify the calculations in the propagation step of the hydrogen-bonding mechanism, 1-amino-1-oxopropan-2-yl-2-hydroxylpropanoate was used to model the adenine end-capped lactide formed in the initiation step.

Results & discussion

Representative examples of the polymerization of L-lactide in bulk in the presence of adenine are given in Table 1. As the reactivity was expected to be low, reactions were first conducted for a L-lactide/adenine ratio of 20. With a L-lactide melting point of around 96 °C, the first experiment was run at 100 °C (entry 1), yielding an extremely low conversion of 1% after 24 h. Substantial to quantitative conversions were obtained for reaction temperatures in the range of 120 to 150 °C (entries 2–4), while a temperature of 180 °C led to degradation of the polymer characterized by a deep brown color (entry 5). Number-average molecular weights up to 5000 g mol^{-1} were obtained, with dispersities in the range of 1.5 to 1.9.

The MALDI ToF analysis of the sample obtained at 120 °C for a L-lactide/adenine ratio of 20 (entry 2) is shown in Fig. 1 (top). The main distribution A corresponds to linear adenine end-capped polylactide with even multiples of 144. As will be seen later, this result from the initiation by the $–NH_2$ group. A minor population corresponding to adenine end-capped polylactide with odd multiples of 144 can also be noticed (a in Fig. 1), highlighting a modest occurrence of intermolecular transesterification. A′ and a′ correspond to the same macromolecular arrangement as A and a, respectively, with the presence of 2 Ag^+ cations instead of one. A very small amount of the macrocyclic species B can be observed, together with small amounts of linear carboxylic acid end-capped polylactide C (even multiple of 144) and c (odd multiple of 144). Increasing the reaction temperature to 135 and 150 °C increases the formation of macrocycles (see the MALDI analysis of entries 3 and 4 in Fig. 1, middle and bottom, respectively).

The infrared spectrum of a typical sample is presented in Fig. 2. Polylactide characteristic stretching frequencies for ν(C=O) and ν(C–O) are represented by the strong band at 1755 cm^{-1} and by the two strong bands between 1300–1000 cm^{-1}, respectively. The characteristic stretching frequencies for $\nu_{as}(CH_3)$ and $\nu_s(CH_3)$ can be seen at 2997 and 2947 cm^{-1}, respectively. Bending frequencies for $\delta_s(CH_3)$ and $\delta_{as}(CH_3)$ have furthermore been identified at 1385 and 1456 cm^{-1}, respectively. The peaks corresponding to ν(C=O–N) and δ(N–H) at 1620 and 1553 cm^{-1} indicated by the arrows in Fig. 2 highlight the presence of a secondary amide group, resulting from the initiation of the polymerization by the $–NH_2$ group.

The ^{1}H-NMR spectrum of a typical adenine end-capped polylactide sample is shown in Fig. 3. The $–CH_3$ (a) and –CH (b) signals of poly(L-lactide) can be seen at 1.46 and 5.21 ppm, respectively. The 4 signals in the 8–13 ppm range are attributed to the adenine chain end, while the ^{1}H NMR signals of adenine in the same zone are shown for comparison. The former were assigned using a COSY analysis reported in Fig. 4. Only one correlation is expected, between protons H8 and H9. Proton H8 is deshielded to 8.44 ppm. The resonance signal of proton H9 appears duplicated, at 12.17 and 12.12 ppm. Adenine and its derivatives are known to exist in several tautomeric forms[44–47] whose relative proportion in solution depends on the nature of the solvent and on the concentration. Proton H2 is deshielded to 8.67 ppm, while the signal at 11.52 ppm is attributed to the amide proton resulting from

Table 1 Polymerization of L-lactide in bulk with adenine at different monomer-to-initiator ratios

Entry	Time (h)	Temp. (°C)	[L-LA]/[Adn]	Conv.[a] (%)	Yield (%)	$M_{n,calc}$[b]	$M_{n,GPC}$[c] (g mol^{-1})	$M_{n,NMR}$[d] (g mol^{-1})	$Đ$[c]
1	24	100	20	1	—	—	—	—	—
2	24	120	20	38	34	1100	2000	2200	1.48
3	24	135	20	71	65	2000	4900	—	1.80
4	24	150	20	95	74	2700	3900	—	1.89
5	24	180	20	84	—		—	—	—
6	24	135	40	34	32	2000	1800	2000	1.36
7	48	135	40	58	58	3500	2900	—	1.53
8	23	135	60	18	18	1700	1300	1500	1.30
9	48	135	60	62	60	5300	3500	—	1.95
10	23	135	100	23	24	3600	2400	—	1.67
11	48	135	100	56	51	7500	4800	—	2.05
12[e]	24	135	20	73	58	2000	2000	2000	1.60

[a] Conversion determined by ^{1}H-NMR. [b] Number-average molecular weight calculated by ([L-LA]/[Adn]) × Conversion × 144 + 135. [c] Number-average molecular weight M_n and dispersity Đ determined by GPC calibrated using polystyrene standards in THF. M_n corrected by a factor of 0.58 for poly(L-lactide).[41] [d] Number-average molecular weight M_n determined by ^{1}H NMR. [e] 4-Aminopyridine was used as an initiator instead of adenine.

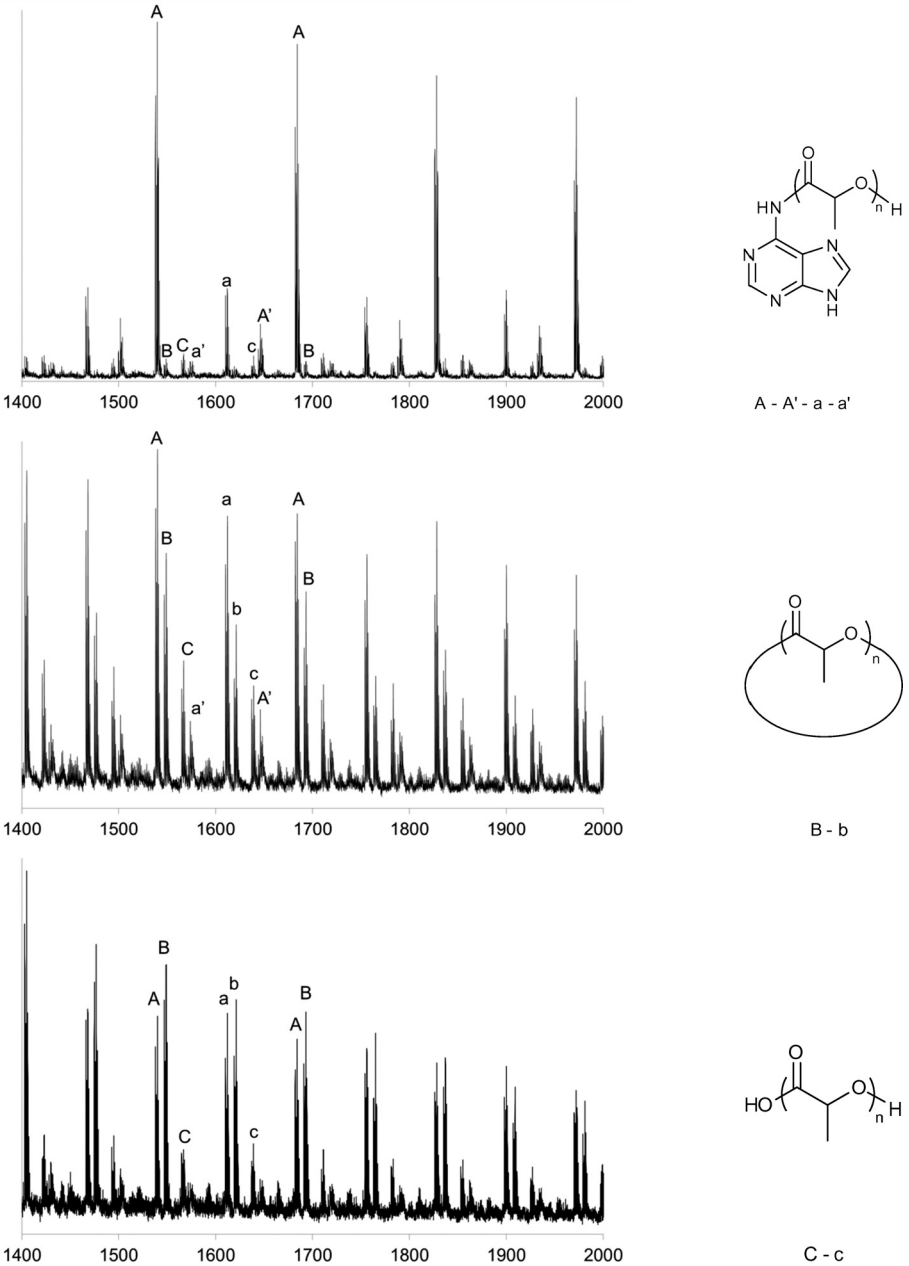

Fig. 1 MALDI ToF spectra of entries 2, 3 and 4 from top to bottom and the structures assigned: adenine end-capped polylactide (A, even and a, odd; A′, even and a′, odd with two Ag^+), macrocycles (B, even; b, odd) and carboxylic acid end-capped polylactide (C, even; c, odd).

the initiation of the ring-opening polymerization by the amine group of adenine.

Further reactions were run for higher L-lactide/adenine ratios at a temperature of 135 °C in order to obtain acceptable conversions. Reactions conducted for 24 h at 135 °C for L-lactide/adenine ratios of 40, 60 and 100 are shown in Table 1 as entries 6, 8 and 10, respectively. Number-average molecular weights in the range of 1300 to 2400 g mol^{-1} are obtained, with dispersities around 1.3 to 1.7. The MALDI ToF spectra of these entries are presented in Fig. 5. Adenine end-capped polylactide is still the major species in all cases, even if substantial amounts of macrocycles can be noticed for a ratio of 100. An increase in the reaction time to 48 h (entries 7, 9 and 11) leads to an increase in the number-average molecular weight and also in the dispersity. The MALDI ToF analyses show in this frame a high proportion of macrocycles, see for example the spectrum for a ratio of 60 in the ESI† (Fig. S1). Homonuclear decoupled ^1H spectra (see Fig. S2†) show that racemization occurs in a modest way in the course of the polymerization of the enantiopure L-lactide.

Conducting the reaction at relatively low temperatures and for short reaction times, *i.e.* 24 h at 120 °C for a ratio of 20 and 24 h at 135 °C for L-lactide/adenine ratios of 40 and 60, affords thus the access to adenine end-capped polylactide in a straightforward one-step procedure (Scheme 2). Number average molecular weights ranging from 1300 to 2000 g mol^{-1}

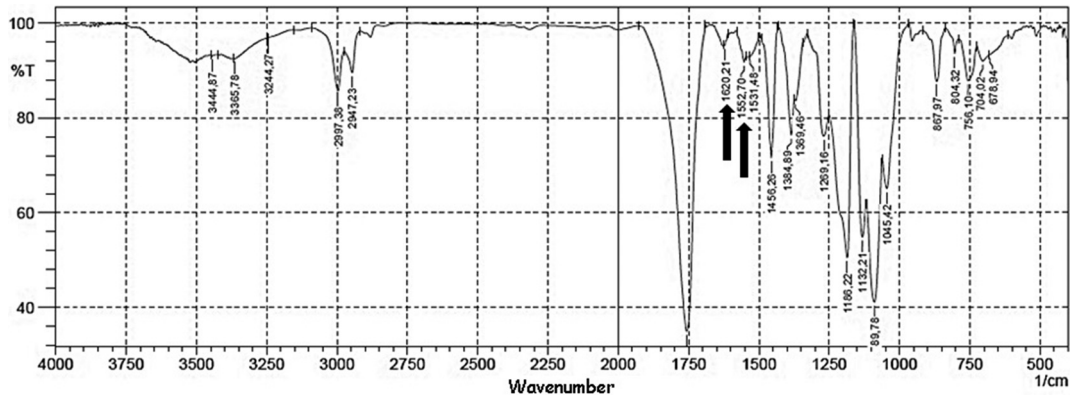

Fig. 2 Representative FTIR spectrum of Adn-PLLA (KBr pellets). Reaction conditions of entry 2.

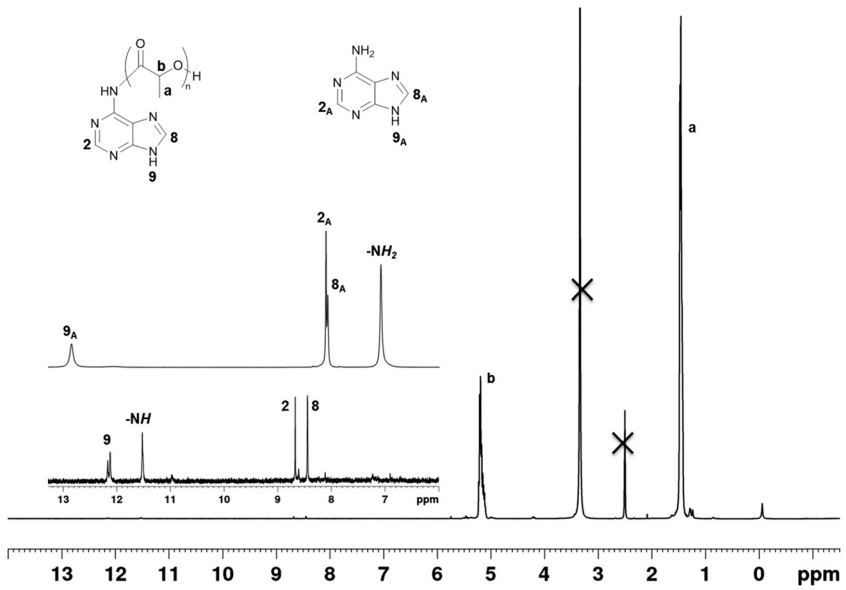

Fig. 3 ^{1}H-NMR spectrum of a typical sample in DMSO-d_6.

and dispersities in the range of 1.3 to 1.5 are obtained. As adenine is not soluble in melted lactide, the initial reactive medium is heterogeneous. Experimentally, it can be seen that the medium becomes homogenous in the course of the polymerization for L-lactide/adenine ratios higher than 20 but not for a ratio of 20. This can be related to the presence of unreacted adenine all along the reaction for a ratio of 20. This partial initiation efficiency leads to experimental number-average molecular weights that are higher than the ones calculated considering the initiation of one macromolecular chain per adenine molecule (entry 2). This is no more the case for higher ratios, where the experimental number-average molecular weights are close to or lower than the calculated ones (entries 6 and 8). It should be noted here that macrocyclic species, observed for certain entries, lower the number-average molecular weight measured by GPC, as cyclic polymers have a lower average size than the corresponding linear polymer with the same degree of polymerization.[48] The presence of unreacted adenine for a ratio of 20 is confirmed by NMR analysis of the reactive medium before quenching, where the signals of adenine can be unambiguously observed (see Fig. S3†). The initiation can thus be considered as quantitative for ratios of 40 and above. Calculated and determined number-average molecular weights are in the same range for entries 6 and 8, and dispersities around 1.30 and 1.36 are obtained. Even if these are typical features of controlled polymerization, this is not the case here *stricto sensu*. Indeed, besides adenine end-capped polylactide, both macrocycles and carboxylic acid end-capped PLA are also formed during the reaction. This is especially the case when high amounts of adenine are used at 135 and 150 °C (entries 3 and 4, MALDI ToF given in Fig. 1) and for long reaction times (entries 9 and 11, MALDI ToF of entry 9 given in the ESI†). This leads to a broadening of the molecular weight distribution.

In order to clarify the reaction mechanism leading to the desired adenine end-capped polylactide, density functional theory (DFT) calculations were performed. Two plausible mechanisms, namely, the nucleophilic mechanism (NM) and

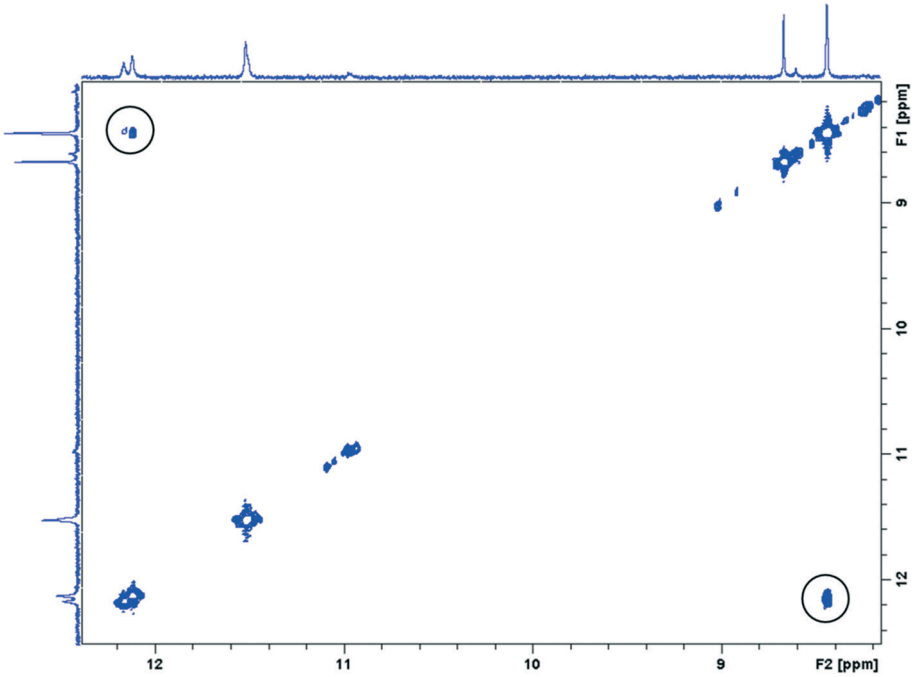

Fig. 4 COSY analysis in the 8–12.5 ppm zone of a typical sample in DMSO-d_6.

the hydrogen-bonding mechanism (HBM) depicted in Scheme 3, can be considered. The NM is based on the well-known covalent-bonding mechanism[32,49–51] which involves a nucleophilic attack of the N-heterocyclic catalyst to the carbonyl group of the ester in the first step. In this mechanism, adenine inserts into the ester group of the L-lactide (**1a**–**2a**), and subsequent hydrogen bonding of the adjacent nitrogen to a second incoming adenine (**3a**) completes the transesterification cycle to form the adenine end-capped polylactide. The HBM was inspired by the mechanism proposed for the triazabicyclodecene (TBD) catalyzed ROP of L-lactide.[51] The previously reported mechanism for TBD catalyzed ROP involves simultaneous activation of the carbonyl group of the ester through hydrogen bonding (to the TBD) along with activation of an initiating alcohol molecule through the interaction of the H of its hydroxyl group with the imine nitrogen of the TBD. In our synthetic approach, we envisaged that adenine acts simultaneously as an initiator and a catalyst of the ring-opening polymerization. Thus, it is hypothesized that, in the first step, the hydrogen attached to the nitrogen of first adenine activates the carbonyl group of the L-lactide through hydrogen bonding, and the imine nitrogen simultaneously activates the amine group of a second adenine by attracting the hydrogen through a lone pair interaction (**1b**). The activated amine group attacks the electrophilic carbon of the carbonyl group of the L-lactide giving an intermediate (**2b**) with a tetrahedral center at this carbon. The subsequent ring opening results in the formation of the adenine end-capped lactide and regeneration of an adenine molecule.

In the computational studies of the TBD catalyzed ROP of L-lactide,[51] where both NM and HBM were studied, the latter was found to be the more plausible. The possibility of catalysis through a hydrogen-bonding mechanism was further supported by experimental work on related reactions[4,52–54] and similar conclusions were found in similar computational analysis for the TBD-catalyzed ring opening of ε-caprolactone.[50] Thus, our studies started with this most plausible mechanism. The energy profile of the initiation step is depicted in Fig. 6, and Scheme 3 shows the proposed mechanism.

The reaction in the initiation step progresses with two transition states. The first step, with a barrier of 24.9 kcal mol^{-1}, is the rate-determining step and corresponds to a catalyzed activated attack of adenine on the carbonyl group of the L-lactide. As hypothesized, the hydrogen attached to the nitrogen of the imidazole ring (H9, in blue, Scheme 3) of the first adenine activates the carbonyl group of the L-lactide through hydrogen bonding (O···H9N bond distance = 1.98 Å), and the imine nitrogen of the pyrimidine ring simultaneously activates the amine group of the second adenine molecule by attracting the hydrogen (in green, Scheme 3) through a lone pair interaction (N···HNH bond distance = 1.99 Å) (**1b**, Scheme 3). The activated amine group thus attack the electrophilic carbon of the carbonyl group of the L-lactide and an intermediate with a tetrahedral center at this carbon is formed (**2b**, Scheme 3) due to the formation of a new single N–C bond (1.46 Å). This is accompanied by an expected increase in the carbonyl C–O bond length (from 1.21 Å to 1.37 Å) and the formation of an O–H bond (0.99 Å). At the same time, a new N–H bond (1.03 Å) is formed due to the transfer of the hydrogen of the activated amine group of the second adenine to the imine nitrogen of the pyrimidine ring of the first adenine. It can be seen in the structure of the formed

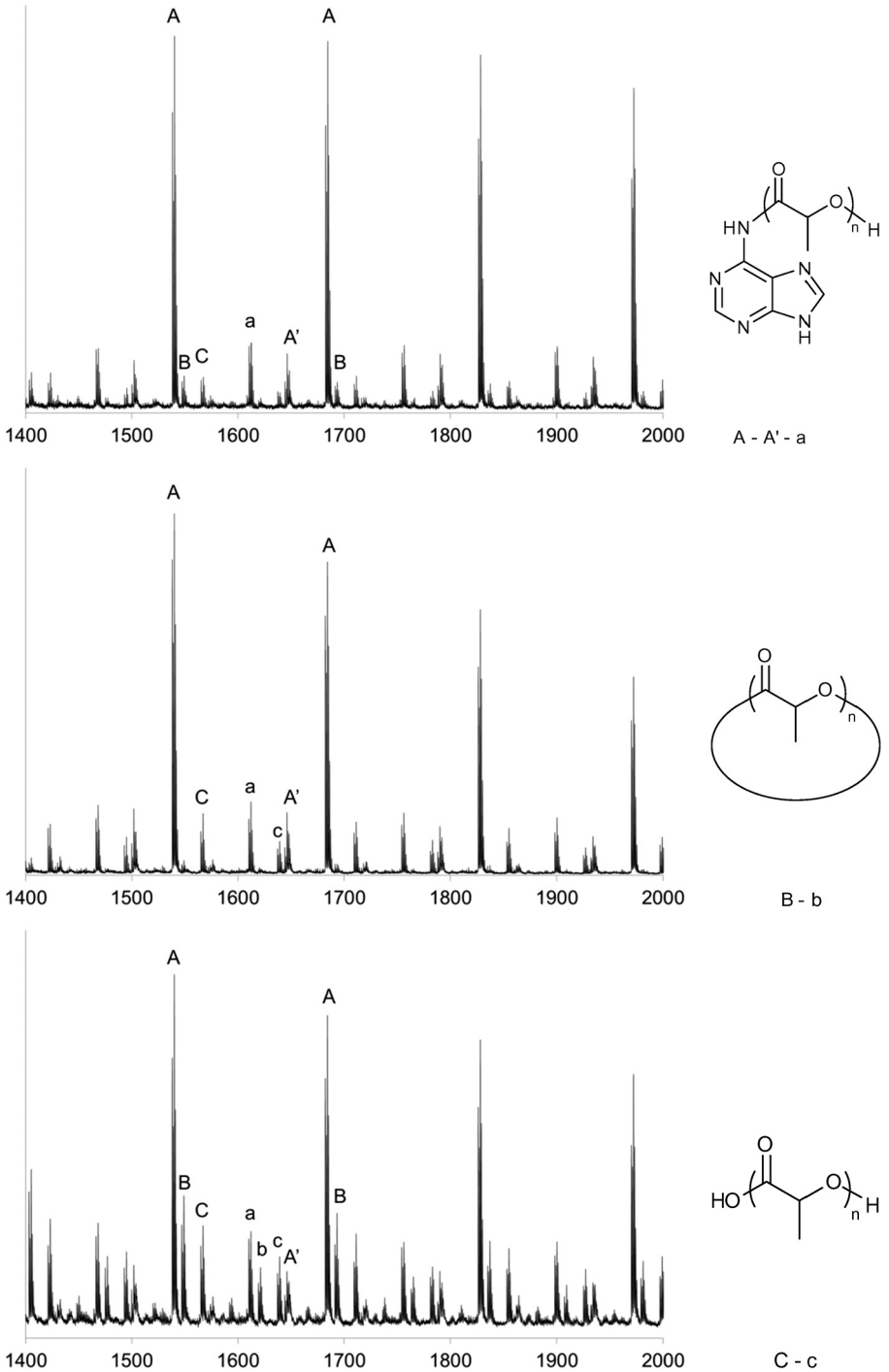

Fig. 5 MALDI ToF spectra of entries 6, 8 and 10 from top to bottom and the structures assigned: adenine end-capped polylactide (A, even and a, odd; A′, even with two Ag^+), macrocycles (B, even; b, odd) and carboxylic acid end-capped PLA (C, even; c, odd).

intermediate that this new bond interacts with the ring oxygen adjacent to the tetrahedral carbon through hydrogen bonding (NH···O bond distance = 1.88 Å). In addition, a hydrogen bonding interaction between the first adenine and the lactide moiety remains, which involves the new O–H bond at the tetrahedral carbon of the lactide and the nitrogen of the imidazole ring of the adenine (OH···N bond distance = 1.85 Å). These two hydrogen bonding interactions constitute the driving force for the subsequent ring opening of the L-lactide moiety, with a considerable lower barrier (12.4 kcal mol^{-1}) than that of the first step. Here, the H (in green, Scheme 3) attached to the imine nitrogen of the pyrimidine ring of the first adenine transfers to the ring oxygen adjacent to the tetrahedral carbon, facilitating the ring opening, and the H (in blue, Scheme 3) of the OH group migrates back to the imidazole ring, thus resulting in the formation of

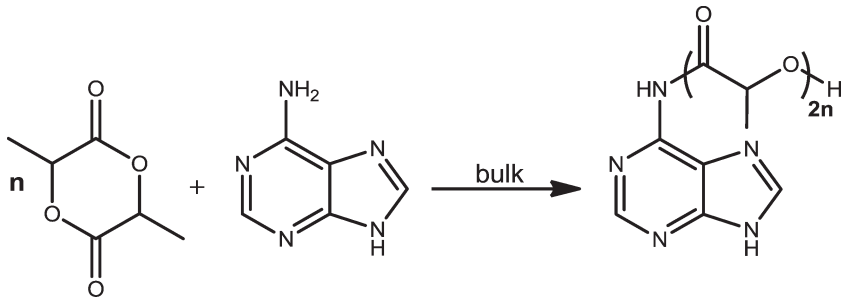

Scheme 2 Access to adenine end-capped polylactide.

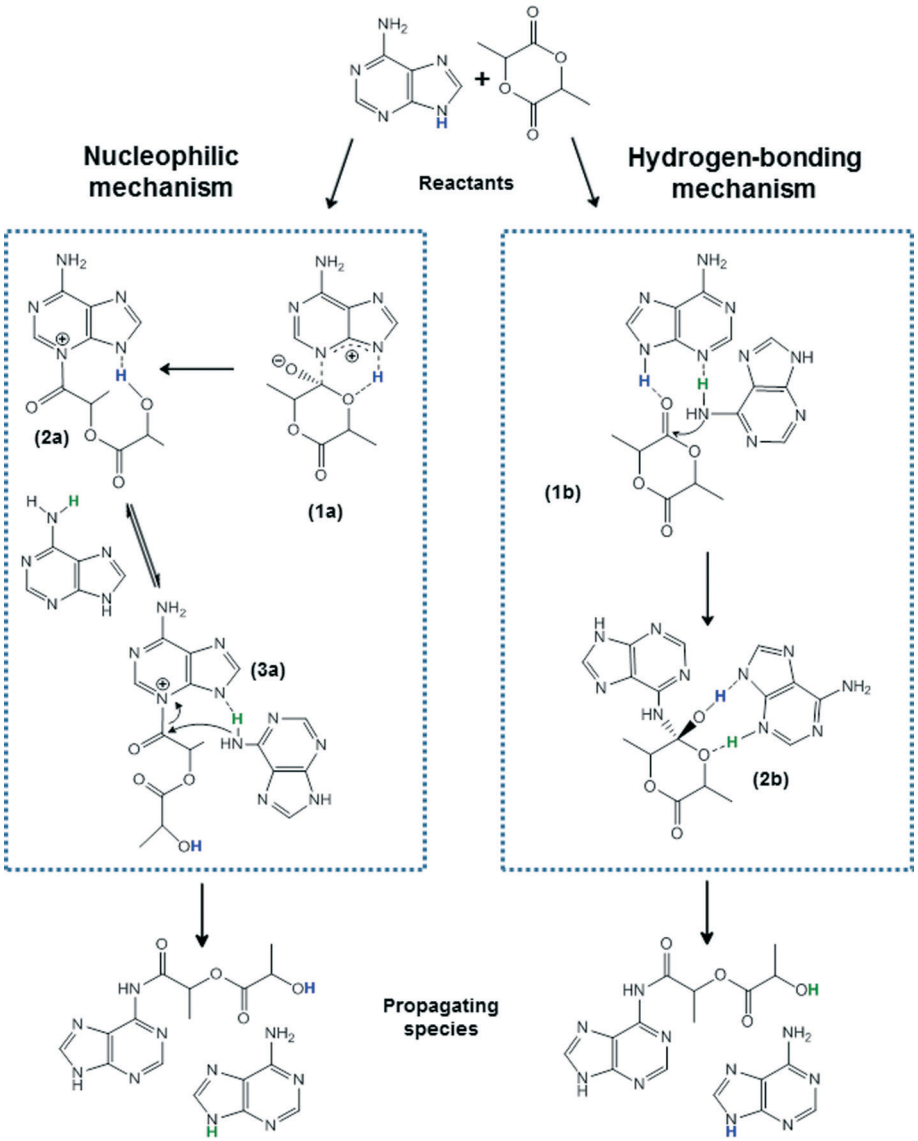

Scheme 3 Initiation steps for the nucleophilic and hydrogen bonding mechanisms.

the adenine end-capped lactide and regeneration of an adenine molecule.

Considering the propagation step, the corresponding energy profile is depicted in Fig. 7, and Scheme 4 shows the proposed mechanism. In order to simplify the calculations, 1-amino-1-oxopropan-2-yl-2-hydroxylpropanoate was used to model the adenine end-capped lactide formed in the initiation step since the purine fragment is not directly involved in this step.

The propagation step of the hydrogen bonding mechanism follows, in general, a similar pattern that was observed

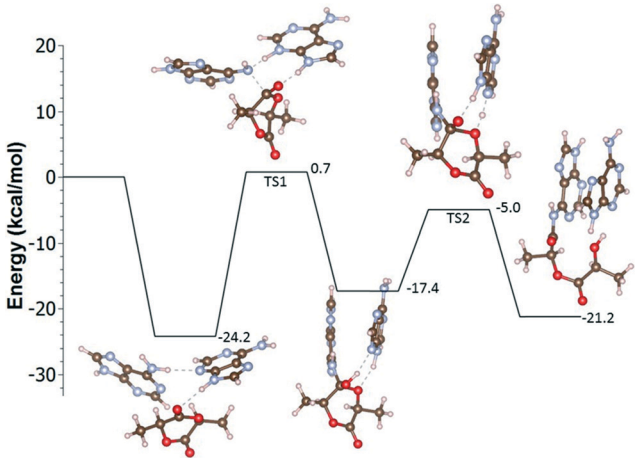

Fig. 6 Energy profile for the initiation step of the hydrogen bonding mechanism.

for the initiation step. The catalyzed activated attack of the adenine end-capped lactide, formed at the end of the initiation step, on the carbonyl group of the L-lactide is very similar to the one in the initiation step. The corresponding energy barrier (16.5 kcal mol^{-1}) is lower than that of the equivalent step in the initiation scheme. In this case, the hydrogen attached to the nitrogen of the imidazole ring (H9, in blue, Scheme 4) of the adenine activates the carbonyl group of the L-lactide through hydrogen bonding (O···H9N bond distance = 1.88 Å), and the imine nitrogen of the pyrimidine ring simultaneously activates the terminal OH group of the adenine end-capped lactide by attracting the hydrogen (in green, Scheme 4) through a lone pair interaction (N···HO bond distance = 1.79 Å) (**2**, Scheme 4). It should be noted that these two hydrogen bonding distances are lower than those of the parent interactions in the first step of the initiation scheme which can favor the subsequent nucleophilic attack of the activated terminal OH group of the adenine end-capped lactide to the carbonyl group of the L-lactide. As a result, an intermediate with a tetrahedral center at this carbon is formed (**3**, Scheme 4) due to the formation of a new single

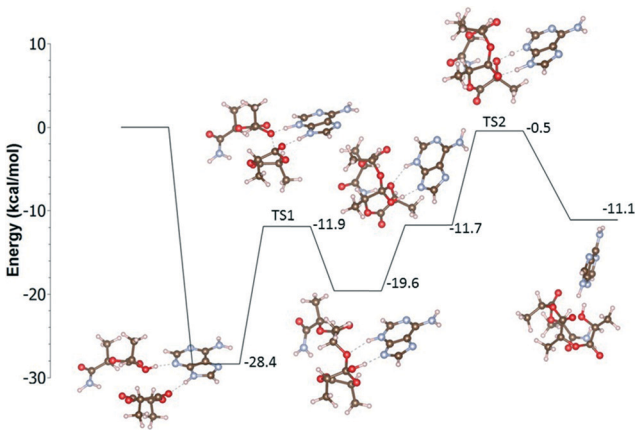

Fig. 7 Energy profile for the propagation step of the hydrogen bonding mechanism.

O–C bond (1.44 Å), which is accompanied by an expected increase in the carbonyl C–O bond length (from 1.21 Å to 1.34 Å) and the formation of an O–H bond (1.02 Å). At the same time, a new N–H bond (1.02 Å) is formed due to the transfer of the hydrogen of the activated OH group of the adenine end-capped lactide to the imine nitrogen of the pyrimidine ring of the adenine. It can be seen in the structure of the formed intermediate that a hydrogen bonding interaction between the adenine and the lactide moiety remains, which involves the new O–H bond at the tetrahedral carbon of the lactide and the nitrogen of the imidazole ring of the adenine (OH···N bond distance = 1.63 Å). In addition, the N–H bond formed retains some hydrogen bonding interaction with the O of the activated OH group that was attached to the carbonyl group of the lactide (NH···O bond distance = 2.00 Å). This intermediate further rearranges and a new structure is formed (**4**, Scheme 4) so that the latter hydrogen bonding interaction vanishes and a new hydrogen bonding interaction between the same N–H bond and the ring oxygen adjacent to the tetrahedral carbon emerges (NH···O bond distance = 2.03 Å). The hydrogen bonding interaction involving the new O–H bond at the tetrahedral carbon of the lactide and the nitrogen from the imidazole ring of the adenine remains with a slight increase in the bond distance when compared to that found in intermediate **3** (OH···N bond distance = 1.67 Å). The higher energy of structure **4** lowers the barrier of the subsequent step in the mechanism that is the ring opening of the lactide moiety (11.2 kcal mol^{-1}). This energy barrier is slightly lower than that of the corresponding ring opening in the initiation scheme (12.4 kcal mol^{-1}). This second step is similar to that in the parent step in the initiation scheme, *i.e.* the H attached to the imine nitrogen of the pyrimidine ring of the adenine transfers to the ring oxygen adjacent to the tetrahedral carbon, facilitating the ring opening, and the H of the OH group migrates back to the imidazole ring, thus resulting in the formation of the adenine end-capped polylactide and regeneration of an adenine molecule (**5**, Scheme 4).

As mentioned above, a different mechanism for the initiation step, the nucleophilic mechanism (NM), for the reaction involving direct covalent binding of the adenine to the carbonyl group of the L-lactide in the first step, as depicted in Scheme 3, could be conceivable and it has also been addressed in our calculations. However, contrary to Rice *et al.* who studied TBD (modeled as guanidine) reacting with L-lactide,[51] we were not able to obtain a transition state for this first step. Probably, the use of the model guanidine in the studies of Rice *et al.* facilitates this step. In our case, in all attempts, a hydrogen bond interaction was formed between the hydrogen attached to the nitrogen of the imidazole ring (H9) of the adenine and the carbonyl group of the L-lactide (O···H9N bond distance = 2.04 Å), similar to that observed in HBM (Fig. 8). This interaction inhibits the desirable hydrogen bond interaction between this N–H9 bond and the oxygen adjacent to the carbonyl group of the lactide and the nucleophilic attack of the imine nitrogen to the carbonyl

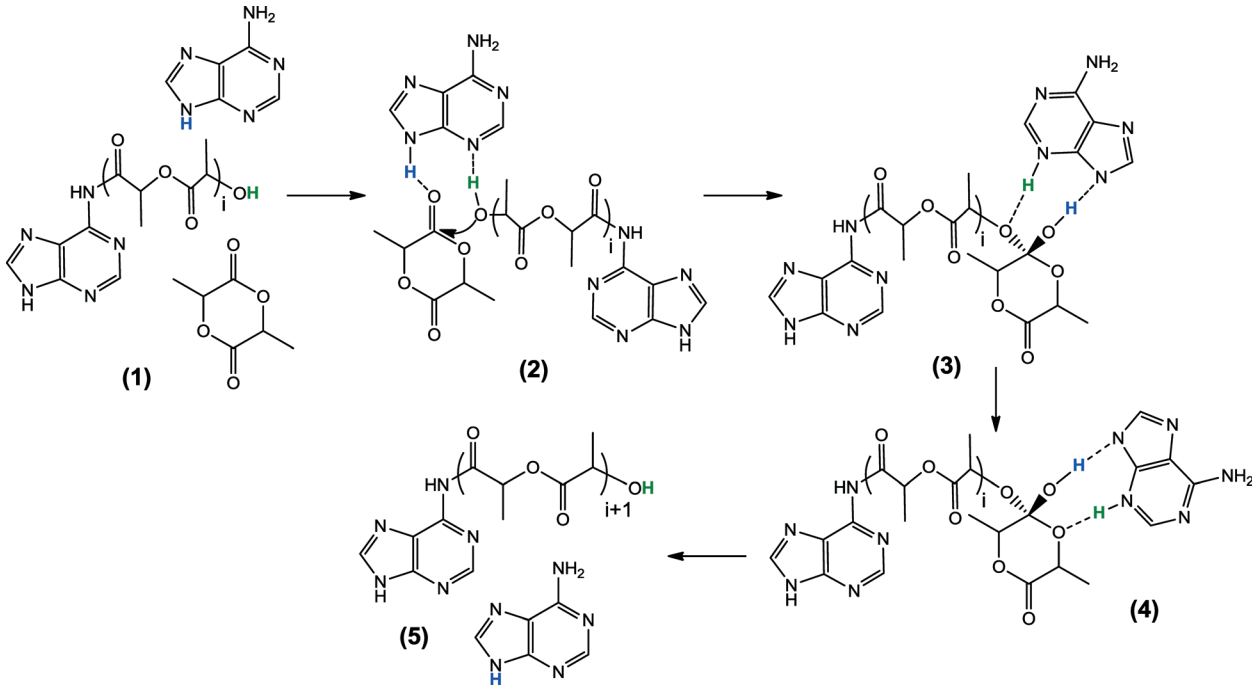

Scheme 4 Propagation step for the hydrogen bonding mechanism.

carbon of the lactide. Accordingly, the insertion of the adenine into the ester group of the L-lactide (**1a**, Scheme 3) does not occur.

Besides the desired adenine end-capped polylactide, both macrocycles and carboxylic acid end-capped polylactide are also formed depending on the reaction conditions. The former can arise either from intramolecular transesterification or by end-to-end cyclisation. In particular, it is well known that imidazoles catalyze the polymerization of lactide, leading to macrocyclic species by end-to-end cyclisation.[34] It is thus conceivable that the formation of the macrocycles observed in this study arises from a similar mechanism catalyzed by the imidazole part of adenine. An experiment was performed using 4-aminopyridine as an initiator (entry 12). The resulting MALDI ToF spectrum shown in Fig. 9 can be compared with that of the polymer obtained using adenine under similar conditions (Fig. 1, middle, corresponding to entry 3). Much less macrocycles are formed when 4-aminopyridine is used as the initiator. Additionally, linear carboxylic acid end-capped polylactide is not formed in the case of 4-aminopyridine, in sharp contrast with adenine. We may thus propose the following. Intramolecular transesterification may occur in the case of 4-aminopyridine, leading to the formation of cyclic species. In the case of adenine, without excluding intramolecular transesterification, the cyclic species formed may arise in a substantial way from the imidazole moiety of adenine. The hydrogen bond between NH9 and the carbonyl group of lactide, predicted in this work by DFT calculations, may lead to the opening of the lactide ring and the subsequent formation of cyclic polylactide as proposed in the literature for imidazole catalysts.[34] The hypothetical mechanism, adapted to adenine from ref. 34, is presented Scheme 5. The hydrolysis of the lactylimidazole active species (3) occurring when quenching the reaction may further lead to linear carboxylic acid end-capped polylactide (5), species that are not observed when 4-aminopyridine is used as the initiator. The hydrolysis of acetylimidazole is known for a long time.[55–57]

Besides the hypothetical mechanism proposed in Scheme 5 to explain the formation of macrocycles, a nucleophilic mechanism involving zwitterionic intermediates can also be conceivable. The zwitterionic ring-opening polymerization (ZROP) as a strategy to generate high molecular weight cyclic polymers has been studied, in particular by R. Waymouth *et al.*[58,59] According

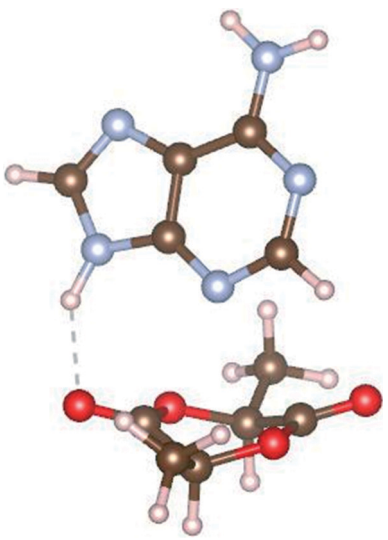

Fig. 8 Adenine–L-lactide adduct showing a hydrogen bonding interaction that disfavors the nucleophilic mechanism.

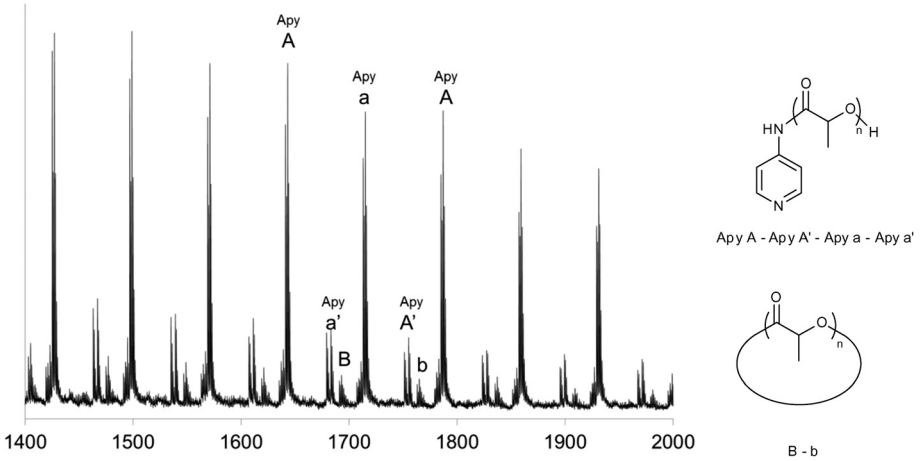

Fig. 9 MALDI ToF analysis of a sample obtained using 4-aminopyridine (entry 13). Structures assigned: 4-aminopyridine end-capped polylactide (Apy A, even and Apy a, odd; Apy A′, even and Apy a′, odd with two Ag^+), macrocycles (B, even; b, odd).

to this mechanism represented Scheme S1, ESI,† the zwitterionic species **1c** can be hypothetically obtained from a direct attack of the adenine to the carbonyl group of the lactide, and the subsequent chain growth by the ZROP mechanism can thus lead to the formation of macrocycles. We envisaged this possibility by DFT calculations. Apart from the fact that the attack of adenine to the lactide would suffer the same problems that were observed for the nucleophilic mechanism discussed above, calculations showed that no stable structure was achieved for the hypothetical zwitterionic species.

Conclusion

Adenine has been assessed as an initiator for the ring-opening polymerization of lactide. The reaction is quantitative under selected experimental conditions. Although transesterification occurs, together with a possible initiation by the imidazole ring of the catalyst leading to macrocyclic species, we have determined conditions that allow a straightforward one-step access to adenine end-capped polylactide, with number-average molecular weights in the range of 1300 to

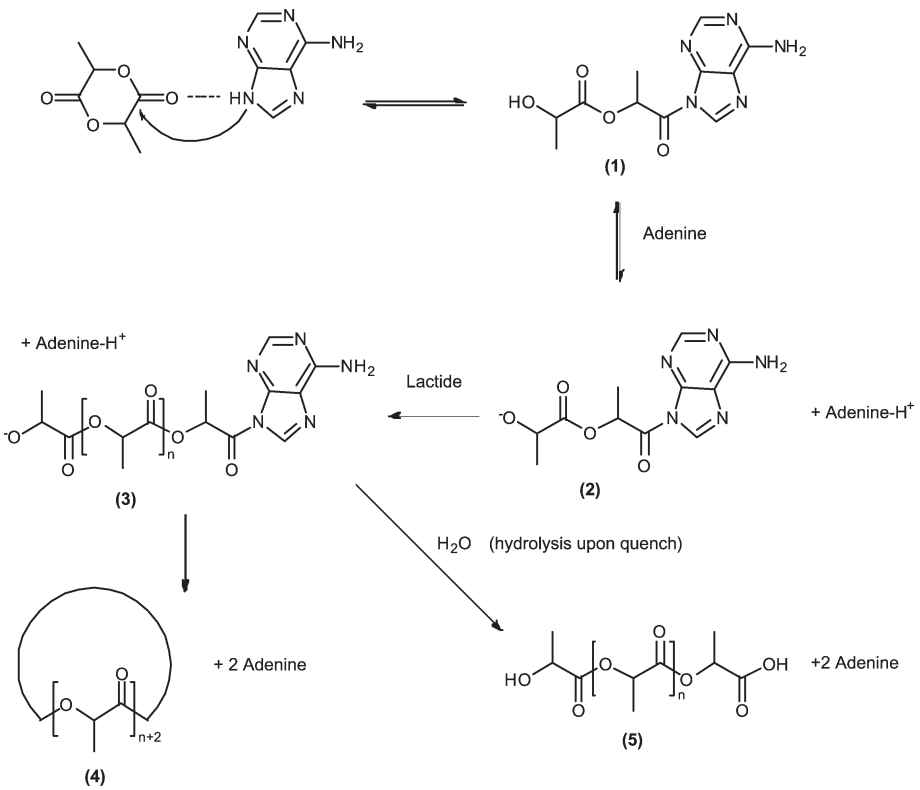

Scheme 5 Hypothetical mechanism for the adenine catalyzed formation of macrocycles and the hydrolysis of lactylimidazole active species leading to carboxylic acid end-capped polylactide.

2000 g mol^{-1} and dispersities in the range of 1.3 to 1.5. A hydrogen bond catalytic mechanism involving a nucleophilic attack of the activated amine group of adenine onto the carbonyl group of lactide is proposed based on DFT studies. Such nucleobase-functionalized biocompatible polyesters are of interest for biomedical applications and will be used as macroligands for the synthesis of new polymer–metal conjugates aiming a better selectivity towards cancer cells.

Acknowledgements

The authors thank the EC Erasmus program for the stay of GN in Lille and the Portuguese Foundation for Science and Technology (FCT) within the scope of the project UID/QUI/00100/2013. Chevreul Institute in Lille (FR 2638), Ministère de l'Enseignement Supérieur et de la Recherche, Région Nord – Pas de Calais and FEDER are also acknowledged for supporting and partially funding this work. AV acknowledges the COST action CM1302 (SIPs) and the *Investigator FCT2013* Initiative for the project IF/01302/2013, as well as the FCT, POPH and FSE – European Social Fund. Aurélie Malfait and Johan Hachani are gratefully acknowledged for their help with GPC and MALDI ToF measurements, respectively.

References

1 N. E. Kamber, W. Jeong, R. M. Waymouth, R. C. Pratt, B. G. G. Lohmeijer and J. L. Hedrick, *Chem. Rev.*, 2007, **107**, 5813–5840.
2 M. K. Kiesewetter, E. J. Shin, J. L. Hedrick and R. M. Waymouth, *Macromolecules*, 2010, **43**, 2093–2107.
3 A. P. Dove, *ACS Macro Lett.*, 2012, **1**, 1409–1412.
4 C. Thomas and B. Bibal, *Green Chem.*, 2014, **16**, 1687.
5 W. N. Ottou, H. Sardon, D. Mecerreyes, J. Vignolle and D. Taton, *Prog. Polym. Sci.*, 2016, **56**, 64–115.
6 P. V. Persson, J. Schröder, K. Wickholm, E. Hedenström and T. Iversen, *Macromolecules*, 2004, **37**, 5889–5893.
7 Y. Miao, Y. Phuphuak, C. Rousseau, T. Bousquet, A. Mortreux, S. Chirachanchai and P. Zinck, *J. Polym. Sci., Part A: Polym. Chem.*, 2013, **51**, 2279–2287.
8 Y. Miao, C. Rousseau, A. Mortreux, P. Martin and P. Zinck, *Polymer*, 2011, **52**, 5018–5026.
9 Y. Phuphuak, Y. Miao, P. Zinck and S. Chirachanchai, *Polymer*, 2013, **54**, 7058–7070.
10 A. Valente, M. H. Garcia, F. Marques, Y. Miao, C. Rousseau and P. Zinck, *J. Inorg. Biochem.*, 2013, **127**, 79–81.
11 C. Peptu, A. Nicolescu, C. A. Peptu, V. Harabagiu, B. C. Simionescu and M. Kowalczuk, *J. Polym. Sci., Part A: Polym. Chem.*, 2010, **48**, 5581–5592.
12 C. Peptu, I. Kwiecien, V. Harabagiu, B. C. Simionescu and M. Kowalczuk, *Cellul. Chem. Technol.*, 2014, **48**, 1–10.
13 Z. Xu, S. Liu, H. Liu, C. Yang, Y. Kang and M. Wang, *Chem. Commun.*, 2015, **51**, 15768–15771.
14 F. Sanda, H. Sanada, Y. Shibasaki and T. Endo, *Macromolecules*, 2002, **35**, 680–683.
15 Y. Takashima, M. Osaki and A. Harada, *J. Am. Chem. Soc.*, 2004, **126**, 13588–13589.
16 M. Osaki, Y. Takashima, H. Yamaguchi and A. Harada, *Macromolecules*, 2007, **40**, 3154–3158.
17 A. Harada, M. Osaki, Y. Takashima and H. Yamaguchi, *Acc. Chem. Res.*, 2008, **41**, 1143–1152.
18 J. Shen, A. Hao, G. Du, H. Zhang and H. Sun, *Carbohydr. Res.*, 2008, **343**, 2517–2522.
19 E. Oledzka, K. Sokolowski, M. Sobczak and W. Kolodziejski, *Polym. Int.*, 2011, **60**, 787–793.
20 S. Sivakova and S. J. Rowan, *Chem. Soc. Rev.*, 2005, **34**, 9.
21 H. J. Spijker, F. L. van Delft and J. C. M. van Hest, *Macromolecules*, 2007, **40**, 12–18.
22 H. S. Bazzi and H. F. Sleiman, *Macromolecules*, 2002, **35**, 9617–9620.
23 B. D. Mather, M. B. Baker, F. L. Beyer, M. A. G. Berg, M. D. Green and T. E. Long, *Macromolecules*, 2007, **40**, 6834–6845.
24 I.-H. Lin, C.-C. Cheng, Y.-C. Yen and F.-C. Chang, *Macromolecules*, 2010, **43**, 1245–1252.
25 D. Wang, Y. Su, C. Jin, B. Zhu, Y. Pang, L. Zhu, J. Liu, C. Tu, D. Yan and X. Zhu, *Biomacromolecules*, 2011, **12**, 1370–1379.
26 A. S. Karikari, B. D. Mather and T. E. Long, *Biomacromolecules*, 2007, **8**, 302–308.
27 K. Zhang, M. Aiba, G. B. Fahs, A. G. Hudson, W. D. Chiang, R. B. Moore, M. Ueda and T. E. Long, *Polym. Chem.*, 2015, **6**, 2434–2444.
28 J. C. Kim, J. Jung, Y. Rho, M. Kim, W. Kwon, H. Kim, I. J. Kim, J. R. Kim and M. Ree, *Biomacromolecules*, 2011, **12**, 2822–2833.
29 K. Yamauchi, J. R. Lizotte and T. E. Long, *Macromolecules*, 2002, **35**, 8745–8750.
30 A. A. A. Smith, T. Hussmann, J. Elich, A. Postma, M.-H. Alves and A. N. Zelikin, *Polym. Chem.*, 2012, **3**, 85–88.
31 F. Nederberg, E. F. Connor, M. Möller, T. Glauser and J. L. Hedrick, *Angew. Chem., Int. Ed.*, 2001, **40**, 2712–2715.
32 R. C. Pratt, B. G. Lohmeijer, D. A. Long, R. M. Waymouth and J. L. Hedrick, *J. Am. Chem. Soc.*, 2006, **128**, 4556–4557.
33 B. G. G. Lohmeijer, R. C. Pratt, F. Leibfarth, J. W. Logan, D. A. Long, A. P. Dove, F. Nederberg, J. Choi, C. Wade, R. M. Waymouth and J. L. Hedrick, *Macromolecules*, 2006, **39**, 8574–8583.
34 H. R. Kricheldorf, N. Lomadze and G. Schwarz, *Macromolecules*, 2008, **41**, 7812–7816.
35 V. Katiyar and H. Nanavati, *Polym. Chem.*, 2010, **1**, 1491.
36 O. Coulembier, S. Moins, J.-M. Raquez, F. Meyer, L. Mespouille, E. Duquesne and P. Dubois, *Polym. Degrad. Stab.*, 2011, **96**, 739–744.
37 A. Kowalski, J. Libiszowski, T. Biela, M. Cypryk, A. Duda and S. Penczek, *Macromolecules*, 2005, **38**, 8170–8176.
38 Y. Matsumura and H. Maeda, *Cancer Res.*, 1986, **46**, 6387–6392.
39 S. Gessi, S. Merighi, V. Sacchetto, C. Simioni and P. A. Borea, *Biochim. Biophys. Acta, Biomembr.*, 2011, **1808**, 1400–1412.
40 S. A. Rivkees, H. Barbhaiya and A. P. IJzerman, *J. Biol. Chem.*, 1999, **274**, 3617–3621.
41 A. Kowalski, A. Duda and S. Penczek, *Macromolecules*, 1998, **31**, 2114–2122.

42 M. J. Frisch, G. W. Trucks, H. B. Schlegel, G. E. Scuseria, M. A. Robb, J. R. Cheeseman, G. Scalmani, V. Barone, B. Mennucci, G. A. Petersson, H. Nakatsuji, M. Caricato, X. Li, H. P. Hratchian, A. F. Izmaylov, J. Bloino, G. Zheng, J. L. Sonnenberg, M. Hada, M. Ehara, K. Toyota, R. Fukuda, J. Hasegawa, M. Ishida, T. Nakajima, Y. Honda, O. Kitao, H. Nakai, T. Vreven, J. A. Montgomery Jr., J. E. Peralta, F. Ogliaro, M. Bearpark, J. J. Heyd, E. Brothers, K. N. Kudin, V. N. Staroverov, R. Kobayashi, J. Normand, K. Raghavachari, A. Rendell, J. C. Burant, S. S. Iyengar, J. Tomasi, M. Cossi, N. Rega, J. M. Millam, M. Klene, J. E. Knox, J. B. Cross, V. Bakken, C. Adamo, J. Jaramillo, R. Gomperts, R. E. Stratmann, O. Yazyev, A. J. Austin, R. Cammi, C. Pomelli, J. W. Ochterski, R. L. Martin, K. Morokuma, V. G. Zakrzewski, G. A. Voth, P. Salvador, J. J. Dannenberg, S. Dapprich, A. D. Daniels, Ö. Farkas, J. B. Foresman, J. V. Ortiz, J. Cioslowski and D. J. Fox, *Revision D.01*, Gaussian, Inc., Wallingford, CT, 2009.
43 Y. Zhao and D. G. Truhlar, *Theor. Chem. Acc.*, 2008, **120**, 215–241.
44 M. T. Chenon, R. J. Pugmire, D. M. Grant, R. P. Panzica and L. B. Townsend, *J. Am. Chem. Soc.*, 1975, **97**, 4636–4642.
45 N. C. Gonnella, H. Nakanishi, J. B. Holtwick, D. S. Horowitz, K. Kanamori, N. J. Leonard and J. D. Roberts, *J. Am. Chem. Soc.*, 1983, **105**, 2050–2055.
46 C. Fonseca Guerra, F. M. Bickelhaupt, S. Saha and F. Wang, *J. Phys. Chem. A*, 2006, **110**, 4012–4020.
47 T. Bartl, Z. Zacharová, P. Sečkářová, E. Kolehmainen and R. Marek, *Eur. J. Org. Chem.*, 2009, **2009**, 1377–1383.
48 D. E. Niehaus and C. Jackson, *Polymer*, 2000, **41**, 259–268.
49 S. Csihony, D. A. Culkin, A. C. Sentman, A. P. Dove, R. M. Waymouth and J. L. Hedrick, *J. Am. Chem. Soc.*, 2005, **127**, 9079–9084.
50 L. Simón and J. M. Goodman, *J. Org. Chem.*, 2007, **72**, 9656–9662.
51 A. Chuma, H. W. Horn, W. C. Swope, R. C. Pratt, L. Zhang, B. G. G. Lohmeijer, C. G. Wade, R. M. Waymouth, J. L. Hedrick and J. E. Rice, *J. Am. Chem. Soc.*, 2008, **130**, 6749–6754.
52 E. J. Corey and M. J. Grogan, *Org. Lett.*, 1999, **1**, 157–160.
53 W. Ye, J. Xu, C.-T. Tan and C.-H. Tan, *Tetrahedron Lett.*, 2005, **46**, 6875–6878.
54 T. Okino, Y. Hoashi, T. Furukawa, X. Xu and Y. Takemoto, *J. Am. Chem. Soc.*, 2005, **127**, 119–125.
55 W. P. Jencks and J. Carriuolo, *J. Biol. Chem.*, 1959, **234**, 1272–1279.
56 B. J. Gour-Salin, *Can. J. Chem.*, 1983, **61**, 2059–2061.
57 T. H. Fife, *Acc. Chem. Res.*, 1993, **26**, 325–331.
58 H. A. Brown, A. G. De Crisci, J. L. Hedrick and R. M. Waymouth, *ACS Macro Lett.*, 2012, **1**, 1113–1115.
59 H. A. Brown and R. M. Waymouth, *Acc. Chem. Res.*, 2013, **46**, 2585–2596.